Advances in Science and Technology Research Journal, 2026, 20(1), 423–435 https://doi.org/10.12913/22998624/211379 ISSN 2299-8624, License CC-BY 4.0 Received: 2025.08.28 Accepted: 2025.10.01 Published: 2025.11.21

Comparative analysis of cross-wedge rolling methods

Zbigniew Pater¹, Janusz Tomczak¹, Xuedao Shu², Zixuan Li²

- ¹ Lublin University of Technology, ul. Nadbystrzycka 36, 20-618 Lublin, Poland
- ² Ningbo University, Fenghua Rd. No. 818, 314211 Ningbo, China
- * Corresponding author's e-mail: z.pater@pollub.pl

ABSTRACT

Flat, convex and concave wedge tools can all be used in cross-wedge rolling (CWR) processes. However, using concave tools requires a new generation of rolling mills with segmented tool assemblies. This paper presents the concepts for such a machine. Next, the influence of tool shape on the CWR process is analysed using the example of a stepped shaft. This analysis was based on numerical simulations carried out using the Simufact.Forming software. The distributions of temperature, effective strain and damage function, as well as force and energy parameters, were compared. Based on this analysis, the most effective CWR process variant was selected.

Keywords: stepped shaft, cross wedge rolling, tools, FEM.

INTRODUCTION

Cross-wedge rolling (CWR) is a widely known method for hot working steel shafts and axles, as well as preforms for die forging [1–3]. However, thanks to numerous research works carried out in recent years, the area of application of the CWR process has been extended to:

- forming of hollow parts, both free [4–6] and on a mandrel [7–9];
- rolling of parts made of non-ferrous materials such as aluminium alloys [10–12], titanium alloys [13–15], magnesium alloys [16, 17] and nickel superalloys [18];
- rolling of hybrid parts from charges welded onto a cylindrical surface [19–21], assembled coaxially [22–24] and butt-welded [25, 26];
- warm rolling [27–29], which is carried out at a temperature lower than the recrystallization temperature and at the same time higher than the ambient temperature;
- forming of large-sized products [30–32], classic examples of which are railway axles.

Numerical modelling played an important role in research aimed at developing CWR technology [33]. The numerical simulations of the

CWR process were mainly based on commercial software dedicated to the analysis metal forming processes, such as Simufact.Forming [34–36], Deform-3D [37–39], Forge [40–42] and QForm [43–45]. In addition to expanding the technological capabilities of the CWR process, researchers developed new methods for this forming process and modernised wedge tools. Among other things, a reversible flat wedge rolling mill was developed at the Lublin University of Technology [46, 47], in which the idle return movement of the tools was eliminated. This machine was used to manufacture balls made from worn railway rail heads. It was also proposed to form parts using sets of segmented tools [48] connected in a caterpillar shape, which can be flat, concave or convex in the working part. Regarding wedge tools, research was aimed at introducing changes that would limit the occurrence of phenomena restricting the CWR process, such as uncontrolled slippage, narrowing (breaking) of the workpiece and the formation of internal cracks [49]. The use of tools with a shaped (convex or concave) wedge-forming surface is particularly interesting in this respect [50].

Given that several basic CWR methods are in use, it was decided to conduct comparative tests of

these methods to determine which is the most effective. The comparison covered three CWR methods, i.e. forming with flat wedges, two rollers and concave tools (in a previously unknown variant). A detailed analysis was conducted to examine the impact of the CWR method on the distribution of strain, temperature and damage functions in the workpiece, as well as its effect on the force and energy parameters of the forming process. Due to cost constraints, the research was limited to thermomechanical analyses. The results of the research presented in this paper may help with the selection of the CWR method when implementing this modern manufacturing technique in industrial conditions.

SUBJECT OF THE STUDY

A comparative analysis was performed using the example of a rolling machine shaft, shown in Figure 1. This part has a maximum diameter of Ø125 mm, a length of 1146 mm and a weight of 67.85 kg. The steps with the smallest diameter of Ø72 mm are located at the ends of the shaft. The maximum reduction ratio $\delta = d_0/d$ (where: d_0 - billet diameter, d - diameter of the rolled step) is 1.74 and can be achieved in a single pass of the wedges. Figure 2 shows the basic wedge tool

that should ensure the desired stepped shaft is obtained in the CWR process. This tool is characterised by a spreading angle $\beta=11^\circ$ (smaller angles $\beta=5.5^\circ$ were used only to calibrate the side surfaces of the rolled steps) and a forming angle $\alpha=22^\circ$. With these assumptions, taking into account the dimensions of the shaft, the length of the working zone of the wedge tool was 3100 mm.

To avoid side waste resulting from surface flow of the material [2], the billet shown in Figure 3 was used in the analysed rolling case. This billet has conical ends that prevent the formation of front funnels in the workpiece. However, preparing such a billet requires an additional operation in which the desired conical ends of the billet are formed.

Based on the wedge parameters presented in Figure 2, wedge tools were designed to ensure the implementation of three cases of CWR, in which flat, convex and concave tools are used. These tools are shown in Figure 4. The simplest tools to develop were the flat tools, which were created by adding an entry zone (two guide paths for proper positioning of the billet) and an exit zone (for receiving the rolled shaft) to the base tool. Convex tools were obtained by winding base wedges onto a cylinder with a diameter of Ø1271 mm. Concave tools, on the other hand, were obtained by winding base wedges inside a ring with

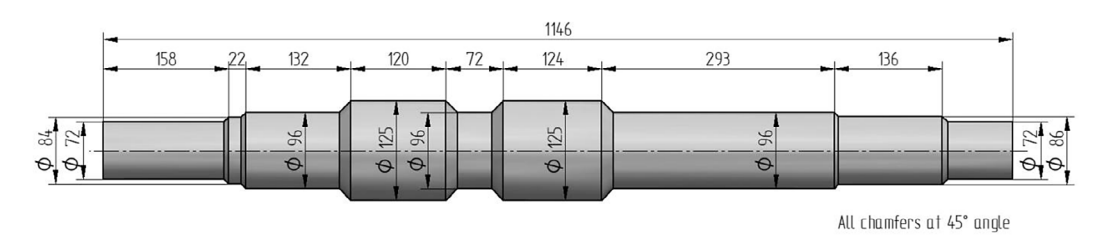


Figure 1. Machine shaft weighing 67.89 kg, subject of analysis

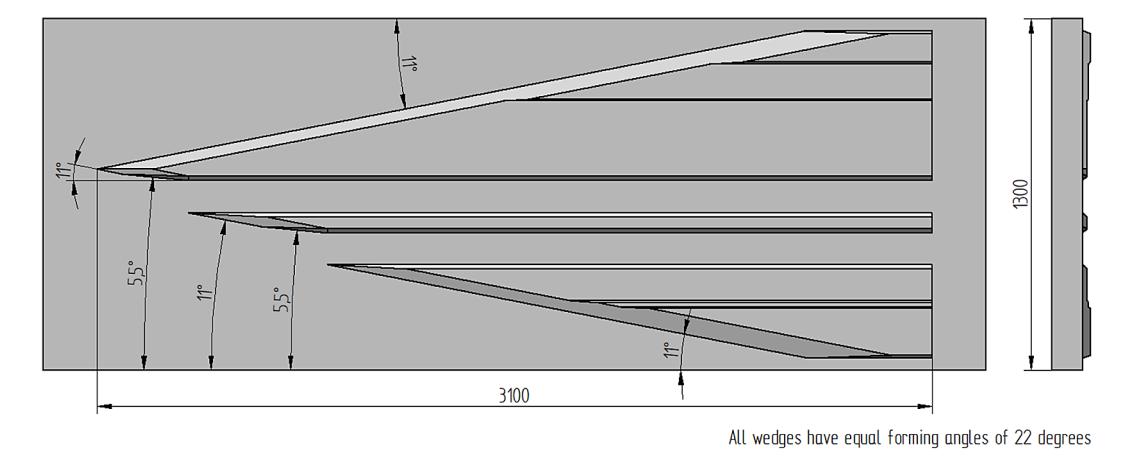


Figure 2. Geometry of wedge tools used for rolling a machine shaft

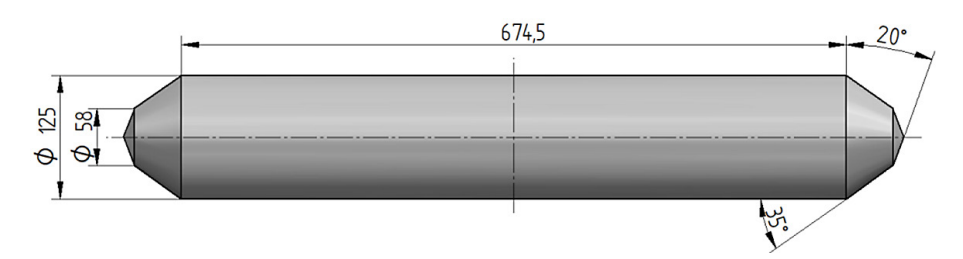


Figure 3. Billet used in the CWR processes of the analysed machine shaft

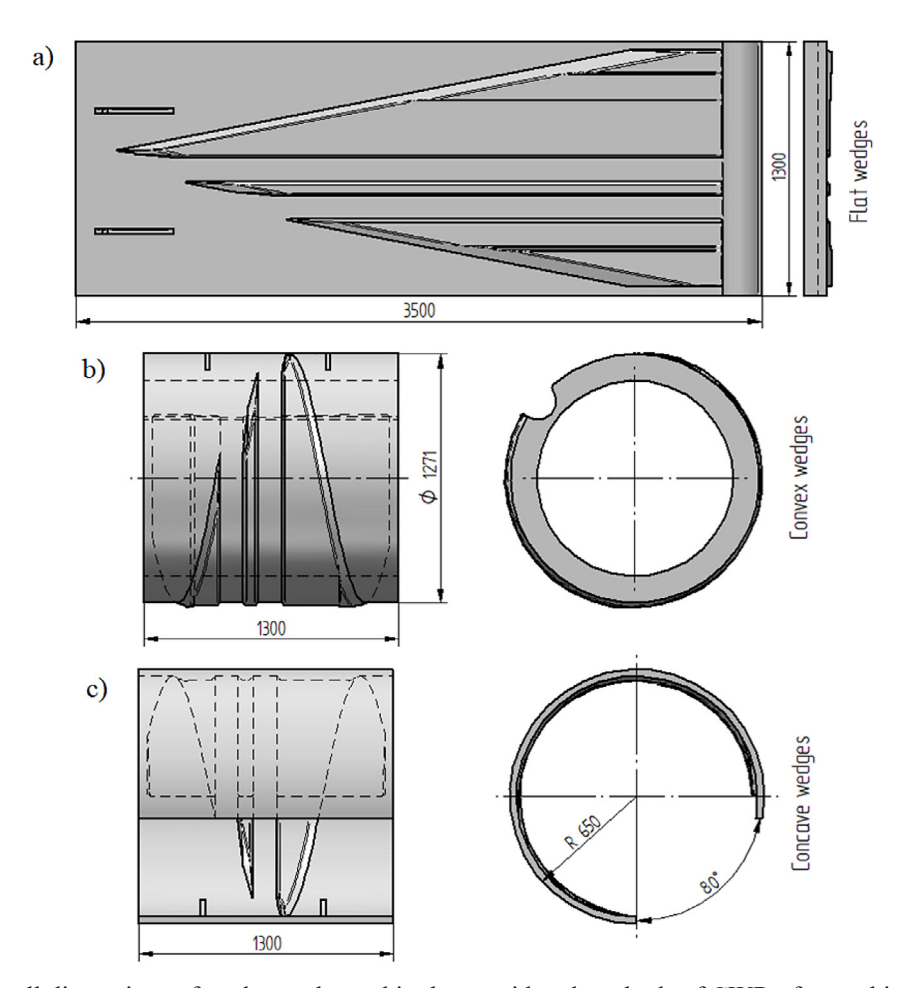


Figure 4. Overall dimensions of wedge tools used in the considered methods of CWR of a machine shaft: a) flat wedge tool, b) convex wedge tool, c) concave wedge tool

a diameter of Ø1300 mm. The tools designed this way were characterised by similar dimensions, which determined the same forming time.

INNOVATIVE ROLLING MILL EXECUTING THE ROLLING PROCESS WITH CONCAVE TOOLS

It is impossible to perform the CWR process using the concave tools shown in Figure 4

because the tools that work together collide. To perform forming with concave tools, therefore, the concave wedge tool must be divided into a series of segments (in the analysed case, 28) which are installed on base plates connected by links to form a tool assembly resembling a caterpillar (Figure 5). The desired concave shape of the tool in the working zone of the rolling mill is achieved by profiling the side surfaces of the base plates appropriately. These plates interlock to form a monolithic tool. This shape is also reinforced by

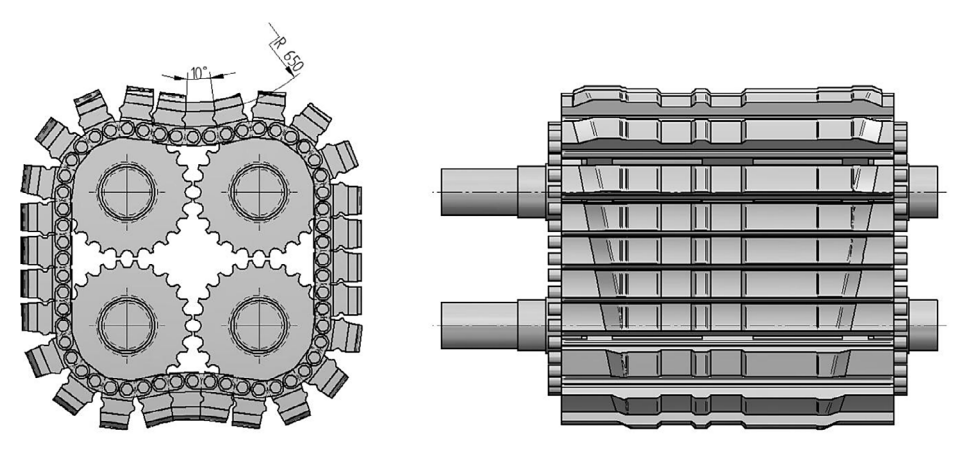


Figure 5. Method of power transmission in a segmented tool assembly characterised by a concave forming surface

placing special guides in the side plates (Figure 6), into which the ends of pins passing through the holes in the links connecting the base plates are inserted. This tool assembly is driven by four identical toothed shafts (see Figure 5).

Figure 7 shows the design of a rolling mill that enables rolling with segmented concave tools. This machine uses two identical tool assemblies, one above the other, whose vertical position can be adjusted using the vertical columns of the rolling mill. The rolling mill drive, which is omitted from Figure 7, is provided by two DC motors, each of which drives four shafts of a given tool assembly (upper or lower) simultaneously. It should be noted that this rolling mill's design concept is innovative on a global scale.

RESULTS OF THE NUMERICAL ANALYSIS

A numerical analysis of three CWR cases was performed using Simufact.Forming. This programme has previously been used to successfully simulate metal forming processes, including cross-wedge rolling [51–53], thick-walled sleeve piercing [54–56], skew rolling of stepped shafts and axles [57–59], and ring rolling [60–62]. The results of the numerical analyses were in very good agreement with those of the experimental tests used to verify them.

Three geometric models of the CWR process of the analysed shaft were constructed using the tools described in the previous section of the

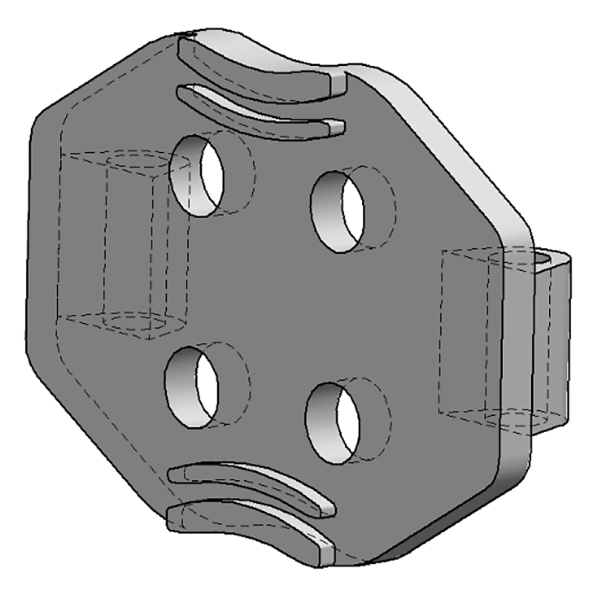


Figure 6. Side plate of the rolling mill with guides (located symmetrically at the bottom and top) for controlling the trajectory of the pins connecting the base plates

article, and are shown in Figure 8. In each case, two identical tools (tool sets), moving in opposite directions, and a billet (see Figure 3) were used. In the case of rolling with two rolls, two guide strips were also used to keep the workpiece within the working zone of the rolls. All tools were treated as perfectly rigid bodies.

Numerical simulations were performed under the assumption that the shaft is made of C45 steel, for which the material model is defined by the following equation [63, 64]:

$$\sigma_F = 2859.8e^{-0.003125T} \varepsilon^{(-0.00004466T - 0.10126)} e^{(-0.00002726T - 0.0008183)/\varepsilon} \dot{\varepsilon}^{(0.00015115T - 0.002748)}$$
 (1)

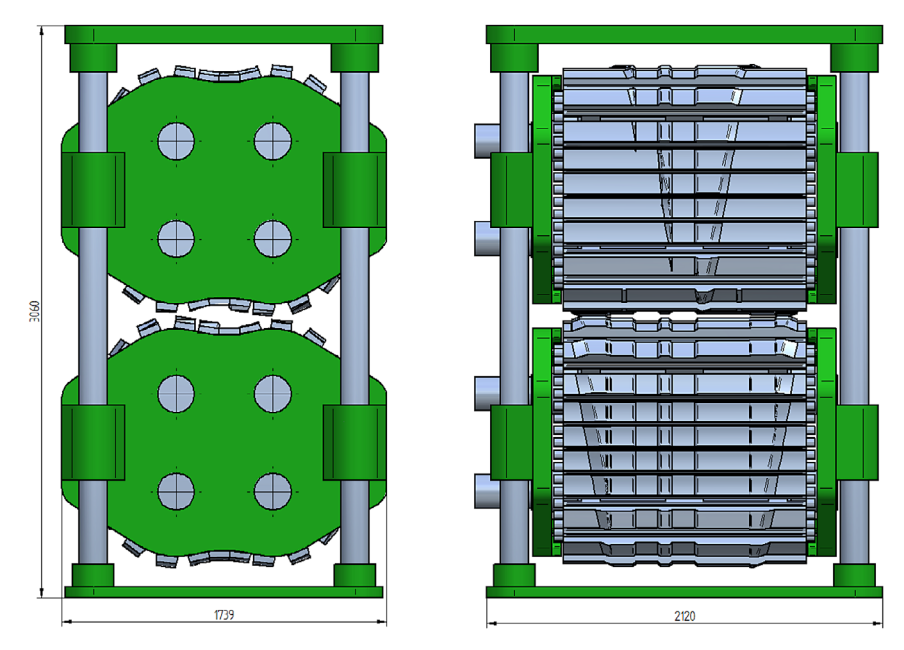


Figure 7. Concept of an innovative segmented rolling mill with concave forming tools

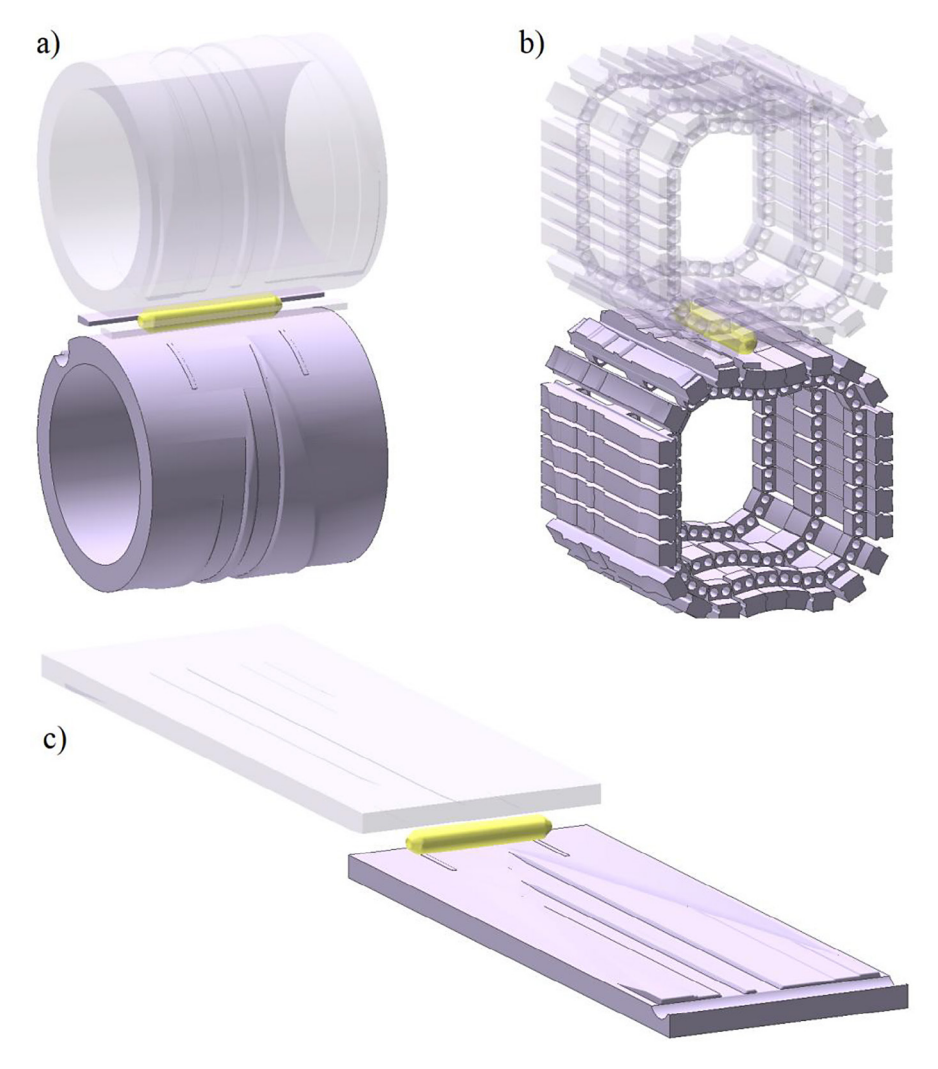


Figure 8. Geometric models of CWR processes in the following configurations: (a) two rolls, (b) concave segments, (c) two flat wedges

where: σ_F is the flow stress, MPa; ε is the effective strain, -; $\dot{\varepsilon}$ is the strain rate, s⁻¹; T is the temperature, °C.

The numerical simulations took into account the thermal phenomena that occur during the forming process. These phenomena are determined by the following parameters: the billet temperature (1,180 °C), the tool temperature (200 °C), and the heat transfer coefficient between the workpiece and the tools (10,000 W/m²K) [63, 64].

The workpiece was modelled using hexahedral solid elements. It was assumed that the size of the elements was 6 mm. Remeshing was used during the calculations when the increase in effective strain in any element exceeded 0.4.

The kinematics of the tools were selected to ensure that the forming cycle took 28 seconds. In the case of rolling with two rolls and sets of concave segment tools, this was the time needed to complete a full rotation of the tools. After the rolled shaft was removed, the tools were ready to start the next production cycle. However, in the case of flat wedges, after rolling and removing the shaft, the tools must be retracted to their starting position to allow the next product to be rolled. Consequently, the productivity of the flat tool forming process is significantly lower than in the other two CWR cases considered.

The contact between the workpiece and the tools was determined by the Tresca friction model, according to which

$$\tau = m k \tag{2}$$

where: τ is the shear stress on contact surface, MPa; m is the friction factor (set equal to m = 0.95 for wedge tools and m = 0.4 for guide rails), -; k is the shear yield stress $(k = \sigma_F/\sqrt{3})$, MPa.

Simulations of three CWR cases for the analysed shaft showed that the correct-shaped product was obtained in each of these processes. All rolling operations were performed stably and no undesirable phenomena, such as uncontrolled slippage or breakage of the workpiece, occurred. Figure 9 shows the CWR process carried out using a set of concave segments. As can be seen from the figure, forming of the shaft proceeds from the centre towards both ends.

Figure 10 shows the temperature distribution in the rolled shaft. Regardless of the CWR method used, the temperature of the material inside the formed product exceeds 880 °C (the appropriate range for hot-temperature steel forming), indicating that the rolling parameters have been correctly selected. In all cases, the temperature of the material in the axial zone of the rolled shaft is higher than in the surface layers. This is undoubtedly due to heat transfer from the workpiece to the much cooler tools. A comparison of the temperature distributions obtained in the CWR cases shows that they are similar. The highest temperatures were recorded in the shaft obtained by rolling with two rolls. This

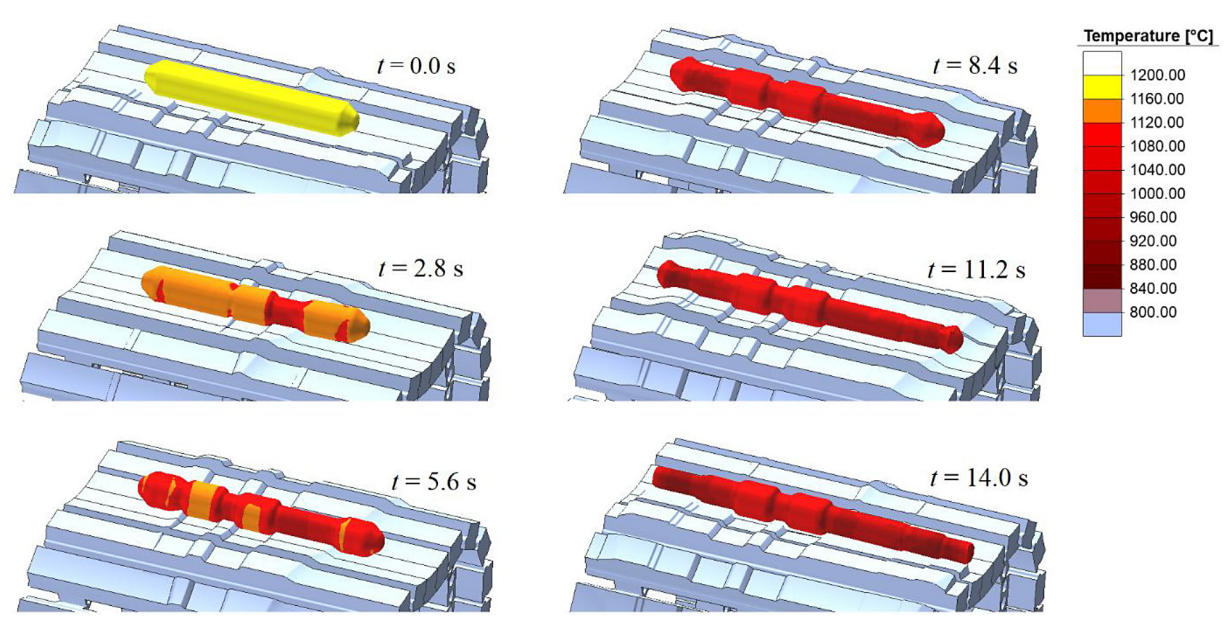


Figure 9. Progression of the shape of the workpiece in the CWR process with concave tool segments and marked temperature distribution (in °C)

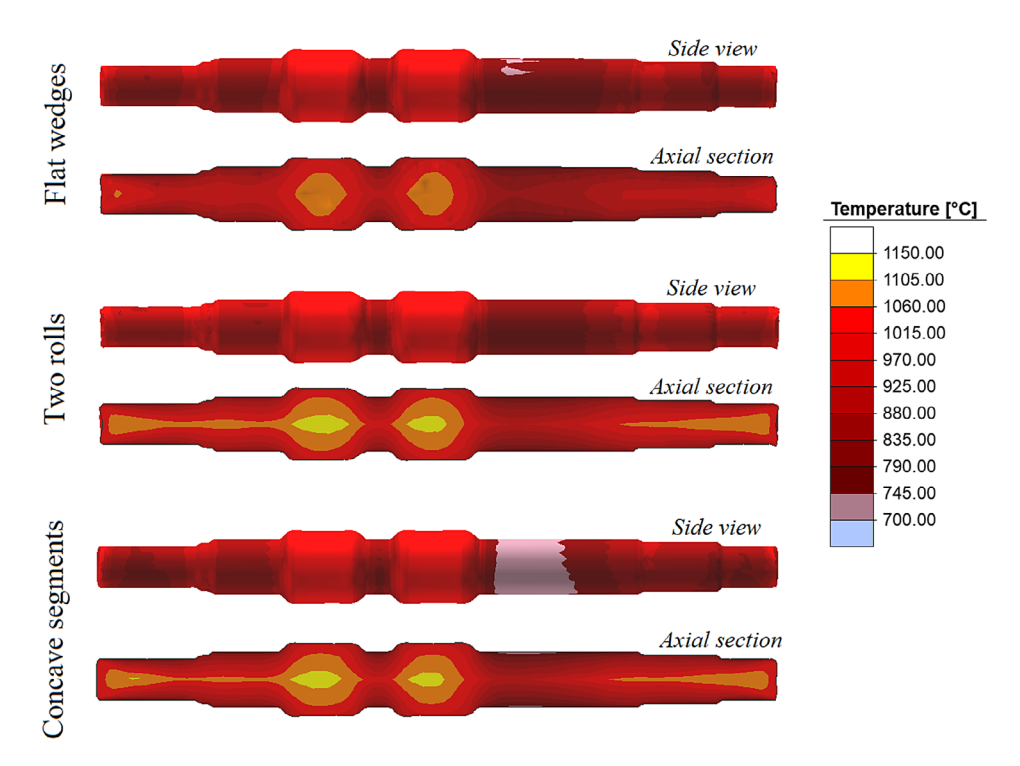


Figure 10. Temperature distributions (in °C) in a rolled stepped shaft, depending on the CWR method used

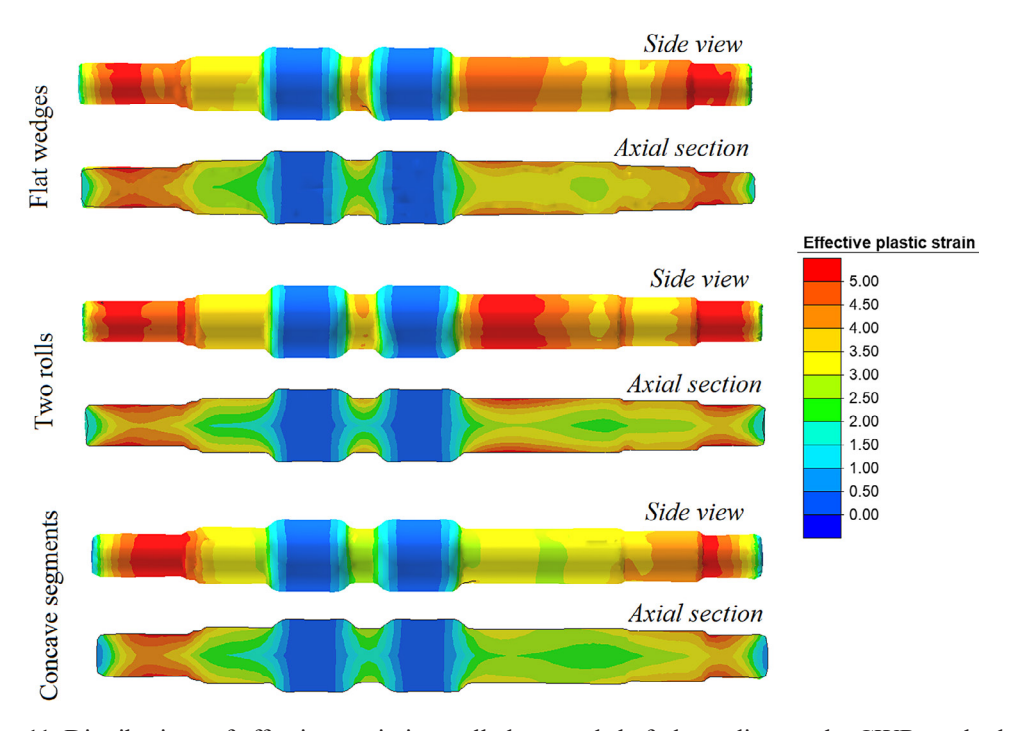


Figure 11. Distributions of effective strain in a rolled stepped shaft depending on the CWR method used

is logical, as the forming value of the contact area between the workpiece and tools is smallest in this case, affecting the amount of heat transferred to the tools.

Figure 11 shows the influence of the CWR method on the distribution of effective strain.

Convergent deformation distributions were obtained in all cases, arranged in rings within the rolled steps of the shaft. The greatest strains occurred in the surface layers due to friction forces causing intense material flow in the

circumferential direction, and the smallest occurred in the axial zone of the workpiece. Interestingly, the analysis of the strain distribution in the long shank of the shaft (on its right side, as shown in Figure 11) reveals further information. The greatest strain was recorded in the shaft formed by two rolls and the smallest in the shaft obtained by rolling with concave segment tools. This appears to be due to differences in ovalisation of the cross-section, which is much greater when rolling with two rolls than with concave tools. Therefore, it can be concluded that the innovative CWR method using segmented concave tools is particularly advantageous for rolling bimetal products where the aim is to minimise the effects conducive to delamination of the workpiece.

One of the fundamental limitations of the CWR process is the tendency for internal cracks to form in the axial zone of the workpiece. The tendency of the material to crack can be monitored by analysing the damage function, which, for the normalised Cockcroft-Latham criterion, is defined by the following relationship:

$$f_{NCL} = \int_0^{\varepsilon_f} \frac{\sigma_1}{\sigma_i} d\varepsilon \tag{3}$$

where: ε_f is critical plastic strain at fracture, σ_i is equivalent stress, σ_1 is maximal principal stress.

The distributions of the f_{NCL} function for the analysed CWR cases are presented in Figure 12. These distributions demonstrate that the highest values of the function are obtained in the outer steps of the shaft with the smallest diameter, regardless of the CWR method used. However, the maximum value of the damage function does not exceed 2.0, meaning it is lower than the critical value of 2.9 determined by [65] for T = 1060 °C, which leads to crack formation.

Numerical simulations were also used to determine the distributions of force and energy parameters in the analysed CWR cases. Figure 13 shows the distribution of the radial force that spreads the cooperating wedge tools. This force causes the rolling mill body to undergo elastic deformation, which affects forming accuracy (the lower the force, the greater the accuracy). Regardless of the method used, the radial force curve was similar in that it increased gradually to reach its maximum value at the end of the forming process. Regarding the maximum radial force value, it should be noted that it is lowest when rolling with two rolls (2,091.4 kN) and

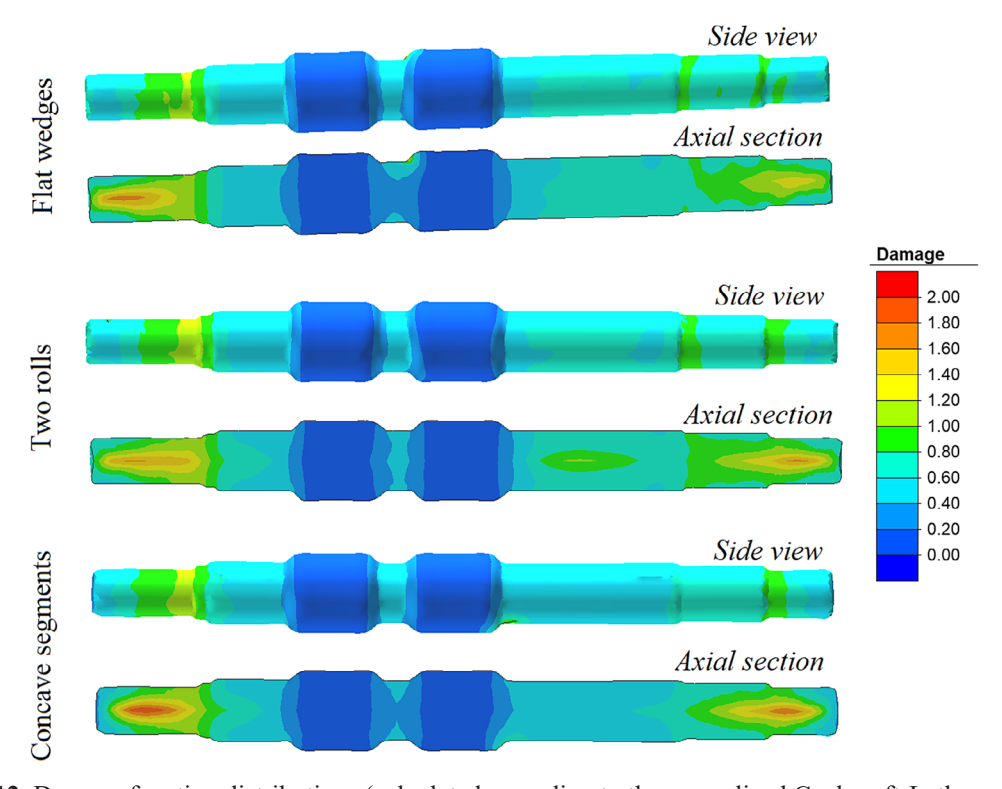


Figure 12. Damage function distributions (calculated according to the normalized Cockcroft-Latham criterion) in a rolled stepped shaft depending on the CWR method used

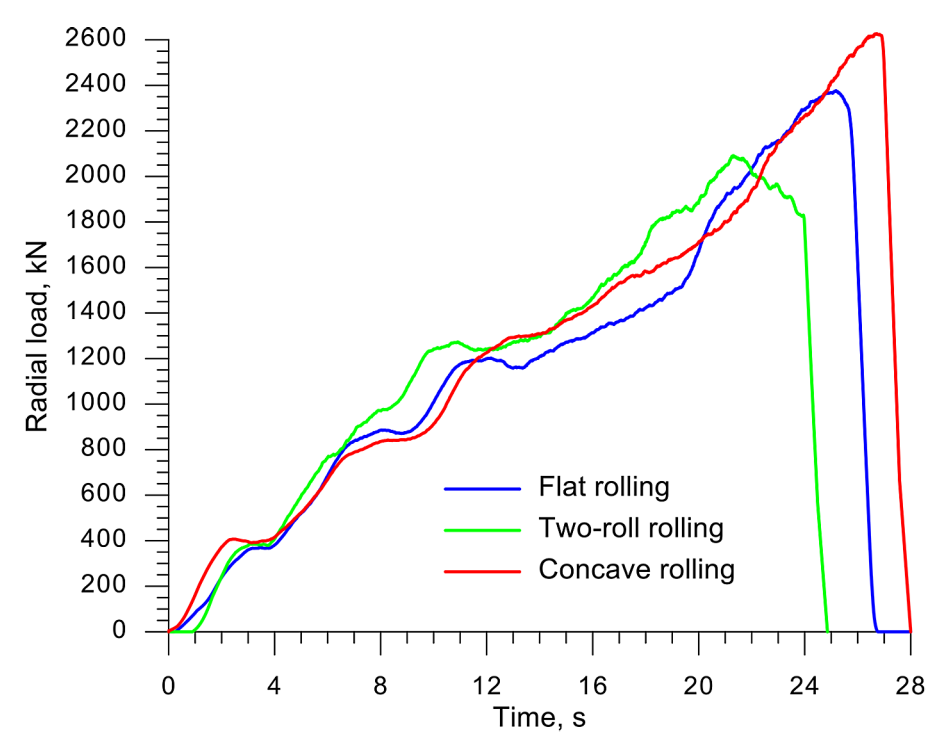


Figure 13. Comparison of radial load distributions acting on the forming tool in the analysed rolling processes

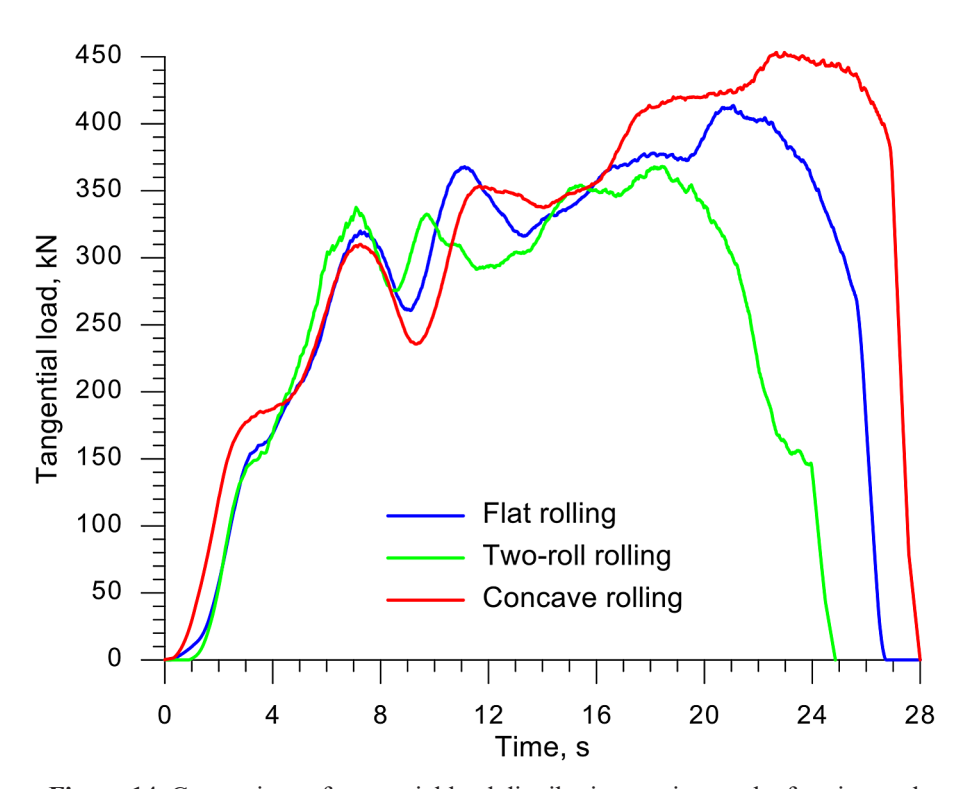


Figure 14. Comparison of tangential load distributions acting on the forming tool in the analysed rolling processes

highest when rolling with concave segmented tools (2,626.7 kN). In the CWR process with flat tools, the maximum radial force is 2,376.4 kN. This difference in maximum radial force values is probably due to differences in the contact area

between the workpiece and the tool. This contact area is largest for concave tools and smallest for convex tools (rolls).

Figure 14 shows the distribution of the tangential force responsible for displacing wedge

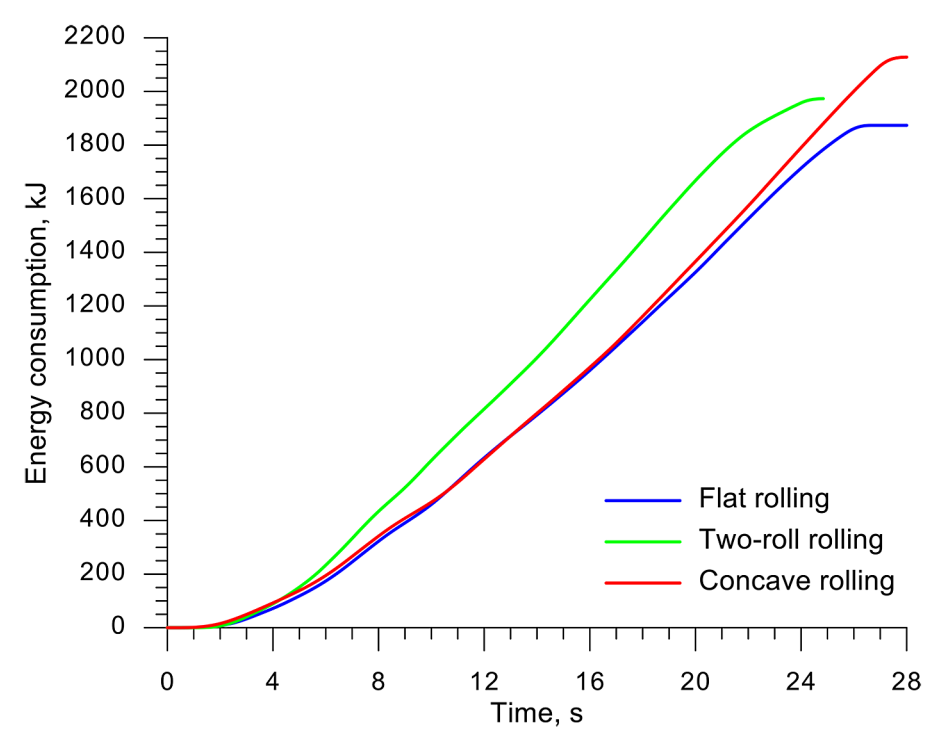


Figure 15. Comparison of energy consumption in the analysed rolling processes

tools, which determines the drive power of the rolling mill. Similar relationships to those observed for the radial force were found for this force. It was shown that the smallest forces occur during rolling with two rolls (where the maximum force is 368.2 kN), intermediate forces occur during CWR with flat tools (413.6 kN), and the maximum forces occur during forming with concave segment tools (453.2 kN). Therefore, the two-roll rolling variant is the most advantageous option in terms of force.

Nowadays, energy consumption is the most important parameter in the forming process. Figure 15 shows the energy consumption curves for the analysed CWR variants. For this parameter, flat wedge rolling was the most advantageous method, with energy consumption amounting to 1,873.6 kJ (100%). Despite lower forming forces, energy consumption was higher for CWR with two rolls and amounted to 1,973.0 kJ (105.3%). The least favourable rolling variant in terms of energy consumption was rolling with concave segment tools, with energy consumption amounting to 2,128.1 kJ (113.6%). In summary, the use of the new concave tool rolling method is not justified in terms of energy consumption.

CONCLUSIONS

Based on the numerical analyses performed, the following conclusions were drawn:

- 1. Axially symmetrical elements, such as stepped shafts and axles, can be manufactured using CWR methods with flat, convex, and concave wedge tools.
- 2. The concept of an innovative rolling mill that enables the forming process to be carried out using concave tool segments was presented.
- 3. The lowest rolling forces occur in the CWR process with two rolls, probably due to the smallest contact area between the workpiece and the tool in this rolling variant.
- 4. Flat wedge rolling is characterised by the lowest energy consumption among the analysed CWR methods, but also has the lowest productivity due to the tools' idle return movement.
- 5. Using the CWR method with segmented concave tools is not justified due to higher force and energy parameters compared to currently used CWR variants. However, this method can be used for special products such as bimetallic or toothed parts.

REFERENCES

- 1. Pater Z. Development of cross-wedge rolling theory and technology. Steel Research International 2010; 81(9): 25–32.
- 2. Pater Z. Cross-Wedge Rolling. In Comprehensive Materials Processing; S.T. Button, Ed.; Elsevier Ltd., 2014; Vol. 3: 211–279.
- 3. Pater Z. Recent developments and future trends in cross wedgerolling. In Comprehensive Materials Processing (Second Edition); 2024; 3: 209–229. https://doi.org/10.1016/B978-0-323-96020-5.00025-X
- Ma J., Yang C., Zheng Z., et al. Influence of process parameters on the microstructural evolution of a rear axle tube during cross wedge rolling. International Journal of Minerals, Metallurgy and Materials 2016; 23(11): 1302–1314. https://doi.org/10.1007/s12613-016-1352-7
- Zheng S., Shu X., Han S., et al. Mechanism and force-energy parameters of a hollow shaft's multiwedge synchrostep cross-wedge rolling. Journal of Mechanical Science and Technology 2019; 33(5): 1–10. https://doi.org/10.1007/s12206-019-0411-1
- Ji H., Liu J., Wang B., et al. Constitutive relationship of 4Cr9Si2 and technological parameters on the inner bore of cross wedge rolling for preform hollow valves. The International Journal of Advanced Manufacturing Technology 2016; 86: 2621–2633. https://doi.org/10.1007/s00170-016-8360-7
- Ji H., Liu J., Wang B., et al. A new method for manufacturing hollow valves via cross wedge rolling and forging: Numerical analysis and experimental validation. Journal of Materials Processing Technology 2017; 240: 1–11. https://doi.org/10.1016/j.jmatprotec.2016.09.004
- Shen J., Wang B., Zhou J., et al. Investigation on the inner hole spiral-groove of cross wedge rolling of hollow shafts with mandrel. The International Journal of Advanced Manufacturing Technology 2020; 110: 1773–1787. https://doi.org/10.1007/ s00170-020-05801-0
- Shen J., Wang B., Yang C., et al. Theoretical study and prediction of the inner hole reduction and critical mandrel diameter in cross wedge rolling of hollow shaft. Journal of Materials Processing Technology 2021; 294: e117140. https://doi.org/10.1016/j. jmatprotec.2021.117140
- 10. Pater Z., Gontarz A., Tofil A. Analysis of the cross-wedge rolling process of toothed shafts made from 2618 aluminium alloy. Journal of Shanghai Jiaotong University (Science) 2011; 16(2): 162–166. https://doi.org/10.1007/s12204-011-1119-2
- 11. Ji Z., Zhou J., Ji J., et al. Influence of tool parameters on internal voids in cross wedge rolling of aluminum alloy parts. Transactions of Nonferrous

- Metals Society of China 2012; 22: 21–26. https://doi.org/10.1016/S1003-6326(12)61678-1
- 12. Wang D., Shu X., Wang R., et al. Mechanism of necking defect of 6082 aluminium alloy rolled by cross-wedge rolling method based on material thermal properties. Journal of Central South University 2020; 27: 3721–3732. https://doi.org/10.1007/ s11771-020-4572-y
- 13. Gontarz A., Pater Z., Tofil A.. Numerical analysis of unconventional forging process of hollowed shaft from Ti-6Al-4V alloy. Journal of Shanghai Jiaotong University (Science) 2011; 16(2): 157–161. https://doi.org/10.1007/s12204-011-1118-3
- 14. Cakircali M., Kichcaslan C., Guden M., et al. Cross wedge rolling of Ti6Al4V (ELI) alloy: the experimental studies and the finite element simulation of the deformation and failure. The International Journal of Advanced Manufacturing Technology 2013; 65: 1273–1287. https://doi.org/10.1007/s00170-012-4256-3
- 15. Li J., Wang B., Ji H., et al. Effects of the cross-wedge rolling parameters on the formability of Ti-6Al-4V alloy. The International Journal of Advanced Manufacturing Technology 2017; 92: 2217–2229. https://doi.org/10.1007/s00170-017-0263-8
- 16. Pater Z., Tomczak J. Experimental tests for cross wedge rolling of forgings made from non-ferrous metals alloys. Archives of Metallurgy and Materials 2012; 57(4): 919–928. https://doi.org/10.2478/ v10172-012-0101-9
- 17. Tomczak J., Pater Z., Bulzak T. Thermo-mechanical analysis of a lever preform forming from magnesium alloy AZ31. Archives of Materials and Metallurgy 2012; 57(4): 1211–1218. https://doi.org/10.2478/v10172-012-0135-z
- 18. Mirahmadi S.J., Hamedi M., Ajami S. Investigating the effects of cross wedge rolling tool parameters on formability of Nimonic® 80A and Nimonic® 115 superalloys. The International Journal of Advanced Manufacturing Technology 2014; 74: 995–1004. https://doi.org/10.1007/s00170-014-6047-5
- 19. Behrens B.A., Overmeyer L., Barroi A., et al. Huskie. Basic study on the process combination of deposition welding and subsequent hot bulk forming. Production Engineering 2013; 7: 585–591. https://doi.org/10.1007/s11740-013-0478-y
- 20. Blohm T., Mildebrath M., Stonis M., et al. Investigation of the coating thickness of plasma-transferred arc deposition welded and cross wedge rolled hybrid parts. Production Engineering 2017; 11: 255–263. https://doi.org/10.1007/s11740-017-0734-7
- 21. Kruse J., Mildebrath M., Behrens B.A., et al. Cross-Wedge Rolling of PTA-Welded Hybrid Steel Billets with Rolling Bearing Steel and Hard Material Coatings. AIP Conference Proceedings 2019; 2113: e040019. https://doi.org/10.1063/1.5112553

- 22. Peng W.F., Zhang J.H., Huang G.X., et al. Stress distributions during the cross-wedge rolling of composite 42CrMo/Q235 laminated shafts. The International Journal of Advanced Manufacturing Technology 2016; 83: 145–155. https://doi.org/10.1007/s00170-015-7541-0
- 23. Wu Z.J., Peng W.F., Shu X.D. Influence of rolling temperature on interface properties of the cross wedge rolling of 42CrMo/Q235 laminated shaft. The International Journal of Advanced Manufacturing Technology 2017; 91: 517–526 https://doi.org/10.1007/s00170-016-9734-6
- 24. Sun B., Xu J., Peng W., et al. Experimental investigation on cross wedge rolling of composite 42CrMo/Q235 laminated shaft. The International Journal of Advanced Manufacturing Technology 2018; 96: 895-903. http://dx.doi.org/10.1007%2Fs00170-017-1537-x
- 25. Kruse J., Jagodzinski A., Langner J., et al. Investigation of the joining zone displacement of cross-wedge rolled serially arranged hybrid parts. International Journal of Material Forming 2020; 13: 517–589. https://doi.org/10.1007/s12289-019-01494-3
- 26. Denkena B., Behrnes B.A., Bergmann B., et al. Potential of process information transfer along the process chain of hybrid components for process monitoring of the cutting process. Production Engineering 2021; 15: 199–209. https://doi.org/10.1007/s11740-021-01023-9
- 27. Huang X., Wang B., Zhou J., et al. Comparative study of warm and hot cross-wedge rolling: numerical simulation and experimental trial. The International Journal of Advanced Manufacturing Technology 2017; 92: 3541-3551. https://doi.org/10.1007/ s00170-017-0399-6
- 28. Bulzak T., Pater Z., Tomczak J., et al. Hot and warm cross-wedge rolling of ball pins Comparative analysis. Journal of Manufacturing Processes 2020; 50: 90–101. https://doi.org/10.1016/j.jmapro.2019.12.001
- 29. Shu X., Shi J., Chen J., et al. Effects of process parameters on surface quality of shaft parts formed by warm cross-wedge rolling. The International Journal of Advanced Manufacturing Technology 2021; 113: 2819–2831. https://doi.org/10.1007/s00170-021-06784-2
- Pater Z., Tomczak J. A new cross wedge rolling process for producing rail axles. MATEC Web of Conferences 2018; 190: e11006. https://doi. org/10.1051/matecconf/201819011006
- 31. Peng W., Sheng S., Chiu Y., et al. Multi-wedge cross wedge rolling process of 42CrMo4 large and long hollow shaft. Rare Metal Materials and Engineering 2016; 45(4): 836–842. https://doi.org/10.1016/S1875-5372(16)30084-4
- 32. Bulzak T. Multi wedge cross rolling of axle

- forgings. Archives of Metallurgy and Materials 2023; 68(2): 697–701. https://doi.org/10.24425/amm.2023.142451
- 33. Pater Z. The application of finite element method for analysis of cross-wedge rolling processes—a review. Materials 2023; 16(13): e4518. https://doi.org/10.3390/ma16134518
- 34. Pater Z. A new approach to numerical modeling of material fracture in cross wedge rolled parts. Journal of Materials Research and Technology 2025; 37: 687–699. https://doi.org/10.1016/j.jmrt.2025.06.047
- 35. Zhu L., Sun Cy., Wang By. et al. Cross wedge rolling deformation law and bonding mechanism of 304 stainless steel/Q235 carbon steel bimetallic shaft. Journal of Iron and Steel Research International 2014; 31: 2423–2437. https://doi.org/10.1007/s42243-024-01300-8
- 36. Wójcik Ł., Bulzak T., Lis K. et al. Rotary compression test for determination of critical value of hybrid damage criterion for railway steel EA1T. International Journal of Material Forming 2024; 17: e28. https://doi.org/10.1007/s12289-024-01827-x
- 37. Shi M., Cheng M., Liu J. et al. Numerical and experimental analysis of defects control in cross wedge rolling for titanium alloy workpieces. The International Journal of Advanced Manufacturing Technology 2024; 134: 3829–3843. https://doi.org/10.1007/s00170-024-14391-0
- 38. Liu J., Shi M., Cheng M., et al. Susceptibility of internal defects to process parameters and control mechanism of defects in cross wedge rolling of Inconel 718 alloy. Journal of Manufacturing Processes 2024; 125: 337–353. https://doi.org/10.1016/j.jmapro.2024.07.045
- 39. Xia Y., Shu X., Zhu D., et al. Effect of process parameters on microscopic uniformity of cross wedge rolling of GH4169 alloy shaft. Journal of Manufacturing Processes 2021; 66: 145–152. https://doi.org/10.1016/j.jmapro.2021.03.063
- 40. Pater Z. Study of cross wedge rolling process of BA3002-type railway axle. Advances in Science and Technology Research Journal 2022; 16(2): 225–231 https://doi.org/10.12913/22998624/147310
- 41. Pater Z., Tomczak, J., Bulzak, T. Novel cross wedge rolling method for producing railcar axles. The International Journal of Advanced Manufacturing Technology 2023; 128: 3403–3413. https://doi.org/10.1007/s00170-023-12142-1
- 42. Pater Z. Numerical simulations of material fracture in cross wedge rolling. Archives of Civil and Mechanical Engineering 2025; 25: e231. https://doi.org/10.1007/s43452-025-01292-6
- 43. Zhou, X., Sun, C., Wang, B. et al. Investigation and prediction of central cracking in cross wedge rolling. The International Journal of Advanced

- Manufacturing Technology 2022; 123: 145–159. https://doi.org/10.1007/s00170-022-10126-1
- 44. Zhou X., Shao, Pruncu Z., et al. A study on central crack formation in cross wedge rolling. Journal of Materials Processing Technology 2020; 279: e116549. https://doi.org/10.1016/j.jmatprotec.2019.116549
- 45. Zhou Z., Shao Z., Zhang C., et al. The study of central cracking mechanism and criterion in cross wedge rolling, International Journal of Machine Tools and Manufacture 2020; 159: e103647, https://doi.org/10.1016/j.ijmachtools.2020.103647
- 46. Tomczak J., Pater Z., Bulzak T. The flat wedge rolling mill for forming balls from heads of scrap railway rails. Archives of Metallurgy and Materials 2018; 63(1): 5–12.
- 47. Pater Z., Tomczak J., Bulzak T. et al. An innovative method for producing balls from scrap rail heads. The International Journal of Advanced Manufacturing Technology 2018; 97: 893–901 (2018). https://doi.org/10.1007/s00170-018-2007-9
- 48. Pater Z., Tomczak J., Shu X., et al. Innovative method of rolling railcar axles using segmented tool assemblies. Advances in Science and Technology Research Journal 2025; 19(3): 271–282. https://doi.org/10.12913/22998624/199778
- 49. Pater Z., Weroński W., Kazanecki J., et al. Study of the process stability of cross wedge rolling. Journal of Materials Processing Technology 1999; 92–93: 458–462. https://doi.org/10.1016/ S0924-0136(99)00229-0
- 50. Pater Z., Tomczak J., Bulzak T. Analysis of the use of variable angular parameter tools in cross-wedge rolling. Journal of Manufacturing Processes 2022; 83: 768–786. https://doi.org/10.1016/j.jmapro.2022.09.052
- Cheng, M., Shi, MJ., Vladimir, P. et al. Novel evaluation method for metal workability during cross wedge rolling process. Advances in Manufacturing 2021; 9: 473–481. https://doi.org/10.1007/s40436-020-00344-9
- 52. Pater Z., Tomczak J., Bulzak T. New forming possibilities in cross wedge rolling processes. Archives of Civil and Mechanical Engineering 2018; 18(1): 149–161. https://doi.org/10.1016/j.acme.2017.06.005
- 53. Jia Z., Wei B., Sun X. Study on the formation and prevention mechanism of internal voids in cross wedge rolling. The International Journal of Advanced Manufacturing Technology 2021; 115: 3579–3587. https://doi.org/10.1007/s00170-021-07367-x
- 54. Lu L., Wang Z., Wang F., et al. Simulation of tube forming process in Mannesmann mill. Journal of Shanghai Jiaotong University (Science) 2011; 16(3): 281-285. https://doi.org/10.1007/s12204-011-1144-1

- 55. Pater Z., Tofil A. FEM simulation of the tube rolling process in Diescher's mill. Advances in Science and Technology Research Journal 2014; 8(22): 51–55. https://doi.org/10.12913/22998624.1105165
- 56. Liu H., Li Q., Gui H. et al. Technology optimization analysis of three-roll rotary piercing process for seamless steel pipe. JOM 2024; 76: 3465–3475. https://doi.org/10.1007/s11837-024-06541-2
- 57. Wang J., Shu X., Ye C. et al. Study on forming quality of three-roll skew rolling hollow axle. The International Journal of Advanced Manufacturing Technology 2023; 128: 1089–1100. https://doi.org/10.1007/s00170-023-11893-1
- Tomczak J., Pater Z., Bulzak T. et al. Design and technological capabilities of a CNC skew rolling mill. Archives of Civil and Mechanical Engineering 2021; 21: e72. https://doi.org/10.1007/s43452-021-00205-7
- 59. Lin L., Yu F., Zhang X. et al. Material modeling and microstructure evolution of LZ50 railway axle steel during bar flexible skew rolling. Archives of Civil and Mechanical Engineering 2025; 25: e63. https:// doi.org/10.1007/s43452-024-01079-1
- 60. Berti G.A., Quagliato L., Monti M. Set-up of radial–axial ring-rolling process: Process worksheet and ring geometry expansion prediction. International Journal of Mechanical Sciences 2015; 99: 58–71. https://doi.org/10.1016/j.ijmecsci.2015.05.004
- 61. Quagliato L., Berti G.A. Mathematical definition of the 3D strain field of the ring in the radial-axial ring rolling process. International Journal of Mechanical Sciences 2016; 115-116: 746–759. https://doi.org/10.1016/j.ijmecsci.2016.07.009
- 62. Lulkiewicz J., Kawałek A., Bajor T., et al. Theoretical analysis of radial-axial ring rolling process of 7075 aluminium alloy. Advances in Science and Technology Research Journal 2024; 18(4): 386–399. https://doi:10.12913/22998624/189901
- 63. Pater, Z., Tomczak, J., Bulzak, T., et al. Assessment of ductile fracture criteria with respect to their application in the modeling of cross Wedge rolling. Journal of Materials Processing Technology. 2020; 278: e116501. https://doi.org/10.1016/j.jmatprotec.2019.116501
- 64. Pater, Z., Tomczak, J., Bulzak, T. Establishment of a new hybrid fracture criterion for cross wedge rolling. International Journal of Mechanical Sciences 2020; 167: e105274. https://doi.org/10.1016/j.ijmecsci.2019.105274
- 65. Pater Z., Tomczak J., Bulzak T., et al. Novel damage calibration test based on cross-wedge rolling. Journal of Materials Research and Technology 2021; 13: 2016–2025. https://doi.org/10.1016/j.jmrt.2021.06.022